Time-domain nuclear magnetic resonance to assess microscale solubility in highly viscous and/or disperse polymer systems

JCIS Open 23 (2026) 100185

Contents lists available at ScienceDirect

JCIS Open

journal homepage: www.journals.elsevier.com/jcis-open

Time-domain nuclear magnetic resonance to assess microscale solubility in highly viscous and/or disperse polymer systems

Joseph U. Okeke [a], Festus Slade [a], Dietmar Obst [b], Diana Bernin [c], Nikolaus Nestle [d,*], Melanie M. Britton [a,**]

[a] School of Chemistry, University of Birmingham, Edgbaston, B15 2TT, UK
[b] BASF Personal Care and Nutrition GmbH, Monheim, Germany
[c] Department of Chemistry and Chemical Engineering, Chalmers University of Technology, Gothenburg, 412 96, Sweden
[d] BASF SE, Carl-Bosch-Strasse 38, Ludwigshafen am Rhein, 67056, Germany

A B S T R A C T

Determination of the physical state of a polymer, whether it is undissolved (solid), as in the case of a microplastic, swollen or fully dissolved, is essential when considering the properties and behaviour of polymeric formulations, but remains challenging within the complex formulations found in many fast moving consumer goods (FMCG). This information is also critical when considering the regulatory controls associated with the application of polymeric formulations. It is, therefore, important to be able to determine and quantify the presence and relative proportion of undissolved polymers within a formulation. Such quantification needs to be simple, rapid and robust for regulatory purposes, but has proved challenging to implement in complex formulations. In this paper, we address this challenge by introducing a novel measure of the degree of solid and undissolved polymer, based on time domain (TD) nuclear magnetic resonance (NMR). Using ^{1}H solid-echo (SE) Carr-Purcell-Meiboom-Gill (CPMG) transverse NMR relaxation curves, we calculate a restricted mobility index, which provides a measure of the proportion of immobile hydrogen atoms present in a sample, arising from solid and undissolved polymeric components within the formulation. Restricted mobility indices are determined for polyvinyl pyrrolidone (PVP), polyquaternium-37 and cellulose polymer formulations as a function or temperature, pH, concentration and processing regime. This method is rapid, easy to implement and does not suffer from the same level of subjectivity as multicomponent fitting or inverse Laplace transforms. The robustness and repeatability of this method is demonstrated across a variety of different TD NMR instruments.

1. Introduction

Natural and synthetic polymers are an indispensable part of daily life, with bulk polymeric materials found ubiquitously in packaging, manufactured components and textiles. However, their application reaches far beyond these most obvious applications and, when dispersed in a solvent, polymers form an essential component of most fast moving consumer good (FMCG) formulations within the pharmaceutical, food, home care and agrochemical industries [1,2]. The personal care industry, for example, uses a range of different cationic polymers in haircare and skincare formulations, because they interact with negatively charged hair and skin surface providing benefits like conditioning or film forming. Thereby, offering application-specific properties, as well as improving product performance. Very often, the degree of dissolution of a dispersed polymer is key to a formulation achieving its desired performance and properties. More broadly, the degree of dissolution of polymers is also critical in their chemical modification and physical transformation processes, such as precipitation spinning [3], as well as their impact on the environment and how their commercial use is regulated. This latter point is of particular significance when considering plastic pollution, for instance, and the difficulties to distinguish between the extreme physical states of dispersed solid polymers (microplastics) and fully dissolved polymers.

Whether a material is solid or liquid is covered by the American Society for Testing and Materials (ASTM) standard D4359-90(2019), which provides a standard test method [4] to determine this. The question of whether a polymer is dissolved or a dispersed solid may seem equally straightforward, and, indeed, has been addressed in many experimental conventions and procedures, such as the Organisation for Economic Co-operation and Development (OECD) guideline 120 [5], which covers the solution/extraction behaviour of polymers in water. However, it remains challenging to distinguish these different physical states for polymers within complex formulations or in technical grade products, due to factors such as turbidity, optical absorption and viscosity. This is especially apparent when taking into account the fact that polymer solubility is often dependant on delicate balances between the

* Corresponding author.
** Corresponding author.
E-mail addresses: nikolaus.nestle@basf.com (N. Nestle), m.m.britton@bham.ac.uk (M.M. Britton).

https://doi.org/10.1016/j.jciso.2026.100185
Received 16 December 2025; Received in revised form 28 April 2026; Accepted 9 May 2026
Available online 11 May 2026

physicochemical conditions within a system. Hence, studies on a neat polymer at pH 7 and low ionic strength, will typically not allow reliable conclusions to be drawn for that polymer within an actual formulation or product. Furthermore, the extraction and isolation of a polymer from a formulation is frequently not practical and almost impossible to achieve without modifying the state of the polymer.

As such, novel approaches for assessing the degree of dissolution for polymers in disperse and complex systems are needed, both for technical reasons, as well as the increasing regulatory interest related to the physical state of polymeric materials. Ideally, such an analytical technique for regulatory purposes should require minimum sample preparation, be robust and easy to implement, as well displaying high sensitivity on a reasonable time scale. Recent work investigating such analytical techniques has focused on dynamic light scattering and small-angle X-ray scattering (SAXS) [6]. However, the use of DLS is limited to optically transparent samples and SAXS requires a high-level of data fitting. An alternative is time domain (TD) nuclear magnetic resonance (NMR), which is able to probe optically opaque, samples. It also benefits from being an established technique already employed in the characterisation of polymeric samples, with a rich history of being utilized in regulatory standards in the pharmaceutical and food industries [7–9]. In TD NMR, low-field magnets are employed that typically possess a magnetic field that is not sufficiently homogeneous to enable molecular identification using the frequency, or 'chemical shift', of the NMR signal, which is more commonly probed in conventional NMR methods [10]. Hence, information is frequently acquired through measurement of T_1 or T_2 NMR relaxation times, known as relaxometry. For assessment of the solid fraction or degree of crystallinity in a sample, ^{1}H T_2 relaxation measurements are often employed, because solid, and particularly crystalline, compounds have significantly shorter relaxation times than the more mobile protons found in amorphous, solvated or liquid molecules [11,12]. In these relaxation measurements, solid echoes (SE) or magic-sandwich echoes (MSE) are typically employed [13], which are able to measure extremely fast T_2 relaxation times, with intense dipolar broadening. While the SE cannot fully refocus dipolar interactions, which the MSE can, the SE is a shorter, simpler sequence, requiring fewer phase cycles than the MSE [12] and is less susceptible to radio-frequency pulse imperfections. As such, sequences based on the SE are considered preferable in industrial and regulatory applications [13]. It has also been shown that comparable signal refocussing is possible, between SE and MSE sequences, in crystalline samples [13,14], particularly where short ($\leq$10 μs) echo spacings are used.

In this study, we propose a novel analytical method for determining the degree of dissolution of polymers within multicomponent formulations, based on proton (^{1}H) transverse NMR relaxation measurements. This approach benefits from being both fast and simple to implement, enabling the assessment of polymeric substances in real formulations, as well as model formulations that mimic the conditions found in real formulations, but which can be controlled and adapted to better understand how they influence the dissolution properties of a polymer. Proton NMR relaxation curves for formulations can be complex, with the full evaluation of data typically requiring multicomponent fits or the inverse Laplace transform [15,16]. Multicomponent fits are, however, sensitive to the choice of model used. The inverse Laplace transform is sensitive to the regularisation parameters selected and suffers from the mathematical instabilities of an ill-posed problem, leading to fitting errors, particularly for curves with poor signal/noise ratio [17]. Yet, the assessment of the dissolved or solid nature of a polymer does not require a full evaluation of the complete curve. Rather a focus of the early time points is required, which are dominated by very short relaxation time components associated with the restricted motion arising from solid or only partially-solvated polymers, and so capture the dissolution state of a polymer. Here, we suggest a simple concept based on the comparison of the averaged signal intensity, over this initial part of the normalized NMR curves, with the expected proton fractions for the polymer within the overall sample.

In this paper, we introduce a *restricted mobility index*, which is able to quantify the degree of undissolved (solid) or partially dissolved polymer within a solution or dispersion. This approach is simple yet robust to implement, as it uses basic mathematical functions, and results in a single number which provides a rapid, and simple to interpret, assessment of the presence and proportion of undissolved (solid) polymers in complex formulations, with minimal data manipulation. We present ^{1}H solid-echo (SE) Carr-Purcell-Meiboom-Gill (CPMG) transverse nuclear magnetic resonance (NMR) relaxation curves for a range of synthetic and natural polymeric solutions. Linear polyvinyl pyrrolidone (PVP), polyquaternium-37 and cellulose polymers were selected to span a diverse range of properties and behaviour, with PVP an example of a well-known fully water soluble polymer and polyquaternium-37 dispersed in oil, as an example of a disperse formulation that undergoes paradoxical changes in macroscopic flow behaviour and optical transparency upon addition of water. Cellulose samples demonstrate the general applicability of the method and its ability to reveal changes in the solubility of this natural polymer caused by sample processing, which is not currently quantifiable using other analytical techniques. The application of this concept is demonstrated as a function of pH, concentration and temperature. The robust nature of our approach is displayed by application of the methodology on multiple low-field NMR instruments at different temperatures.

2. Materials and methods

2.1. Materials

Synthetic polymer-containing formulations were prepared from linear polyvinyl pyrrolidone (PVP), or polyquaternium-37 (polyquat-37). PVP, with a molecular weight of 2.2 MDa, was acquired from BASF and concentrated by water evaporation. Polyquat-37 is commercially available as a white dispersion in an propylene glycol ester oil with a polymer content of approx. 50%. Formulations were prepared over a range of mass fractions through addition of H_2O. An emulsifier was added to the dispersion of oily polyquaternium-37 to assist with mixing in water, over a range of ratios, with the majority of mixing ratios resulting in a macroscopically homogeneous and frequently highly opaque liquid (see Figure SI1 in the Supplementary Information). Samples were allowed to equilibrate over several hours before measurements were performed. Cellulose-containing formulations were prepared using commercial cellulose (MCC Avicel PH-105) from FMC BioPolymer and used without further treatment. These samples are identified as cellulose (MCC) in Figs. 5 and 6. Cellulose derived from Birch (*Betula pendula*) prehydrolysed Kraft pulp was used (intrinsic viscosity = 476 $cm^3\,g^{-1}$; degree of polydispersity = 1133, M_n = 65.9 kDa, M_w = 269.3 kDa, polydispersity index 4.1), which is identified as 'wood 400', in Fig. 7. Birch pulp was also acid hydrolyzed to an intrinsic viscosity of 200 $cm^3\,g^{-1}$ which is identified as 'wood 200', in Fig. 7. Oat husks and wheat straws, received from a farmer in Southern Sweden, were pulped using the Soda Process and bleached. The pulping process included acid pretreatment and cooking in 1.5 L steel autoclaves rotating at 15 rpm within a thermostated polyethylene glycol bath. Ethylenediaminetetraacetic acid chelating and peroxide bleaching were performed in polyethylene bags placed in water baths as described by Wojtasz et al. [18]. After each step the pulp was carefully washed. The resulting pulps contained 96.6 and 96.3% cellulose, 2.1 and 2.3% hemicelluloses and 0.3 and 0.5% Klason lignin, which were acid hydrolyzed with 1 M HCl to reach an intrinsic viscosity of 200 $cm^3\,g^{-1}$. These cellulose samples are identified as 'wheat' and 'oat' in Fig. 7. Samples containing 30% cellulose (MCC) were prepared using either H_2O or D_2O.

Where D_2O was used at high dilution, to maintain a sufficiently high proportion of the NMR signal arising from the polymer fraction, it was observed that the proton relaxation time of the water phase was strongly affected, due to the significantly lower magnetogyric ratio of deuterium

and the subsequent increasing proton-proton distances. However, replacing H_2O with D_2O had a minimal effect on the relaxation times of protons within the polymer, which are typically very short (<100 μs) and are still predominantly influenced by neighbouring hydrogen nuclei within the polymer itself. In the systems studied, the fraction of non-exchanging protons, over the total number of protons, is typically negligible in the synthetic polymers studied here and as high as 30% in the cellulose samples.

2.2. Methods

2.2.1. Time domain NMR

Proton transverse relaxation curves were acquired using a pulse sequence combining a solid echo (SE) with a Carr-Purcell-Meiboom-Gill (CPMG) train, which allows the acquisition of the full transverse relaxation decay in a single experiment. While the signal decay during the solid echo part of the sequence is evaluated in the restricted mobility index, the signal during the CPMG part of the data, which is associated with the transverse relaxation behaviour of the solvent, provides an internal calibration mechanism, which can compensate for any systematic differences between the solid echo decays between different TD-NMR systems (see section S1.2.1 in the Supplementary Information). Furthermore, by combining SE-CPMG sequences, changes in polymer dissolution can be observed simultaneously through complementary changes in the transverse relaxation times for both polymer and solvent protons. Details of this SE-CPMG pulse sequence and its implementation can be found in the supplementary information and elsewhere [19]. The solid echo part of the sequence comprises solid echoes with a fixed echo time of 10 μs (slightly longer than the receiver dead time), with a sampling rate of 250 MHz (Minispec instruments) or 100 MHz (Pure Devices instruments) and the CPMG part of the sequence comprised 8000 echoes with an echo spacing of 240 μs. Relaxation curves were acquired using between 8 and 128 signal averages, depending on the sample and instrument.

Relaxation curves were acquired using multiple low-field, time-domain (TD) Bruker minispec mq20 spectrometers, operating at 20 MHz proton resonance frequency, with variable sample temperatures ranging from −10 °C to 50 °C and a magspec NMR-SCA instrument obtained from Pure Devices (Rimpar, Germany) operating at 24 MHz proton resonance frequency and with a constant sample temperature of 40 °C. For temperature control on the Bruker minispec, an N_2 temperature controller obtained from Bruker was used. For measurements above ambient temperature, it was supplied with nitrogen gas from the building network, for temperatures below ambient, the nitrogen flow was precooled using an XR90 gas cooler obtained from SP Scientific (Stone Ridge NY).

A restricted mobility index (the development of which is described in section 2.2.2) was calculated for each decay curve using the first 100 μs of the solid echo signal and equation (5). As the points at the transition between the solid echo and CPMG regions in the SE-CPMG data decays are affected by hardware imperfections and flip angle variabilities, which are specific to each instrument, it was necessary to correct decays using the method described in the supplementary information (section S1.2.1). This correction was performed on each raw data set, to ensure restricted mobility indices were comparable, regardless of the instrument used to collect the data. Multicomponent fitting was performed using MATLAB [20]. T_2 NMR relaxation times were determined for the water solvent in the PVP samples by plotting the natural logarithm of the signal intensity against time and fitting a trendline over the linear region for these plots, which was typically between 62 ms and 186 ms. It was ensured that the signal used for this measurement arose purely from protons within the water, by selecting a time window that was at longer times than any signal from the polymer protons, which have significantly shorter relaxation times than the water protons. Furthermore, there are no exchangeable protons in PVP.

2.2.2. Restricted mobility index

The restricted mobility index has been developed to quantify the degree of undissolved, and hence restricted mobility, polymer components within a formulation, through a single characteristic value. It is built on a simple approach to compare NMR signal decays, first introduced for unilateral NMR data by Blümich et al. [21], which relies on the ratio between different integral signal "bins". In our approach, we propose using the ratio between the average normalized signal amplitude over the first 15 μs, $\langle s(t)\rangle_{15}$, from the solid echo part of the decay, with the average normalized signal amplitude over the full 100 μs of the acquired solid echo, $\langle s(t)\rangle_{100}$, as the key indicator of the presence of any solid-like polymer, exhibiting restricted mobility (Eq. (1)).

We subtract 1 from the ratio, so that formulations with fully dissolved polymer, which would have negligible decay <100 μs, result in an unnormalized mobility restriction index, x_u, of approximately zero. Formulations with increasing contributions of non-dissolved polymer would result in an increasing value of the mobility restriction index, as the level of signal decay increases below 20 μs, up to an expected maximum value of approximately 5 - 6 for fully rigid polymers with low solvent content.

$$x_u = \frac{\langle s(t)\rangle_{15}}{\langle s(t)\rangle_{100}} - 1 \qquad \text{Eq. 1}$$

Selecting the signal intensity at a time point of 15 μs is motivated by the typical relaxation times expected for rigid polymer components [11]. We observe in fits of the highest concentration PVP and polyquat samples, Gaussian components with relaxation times around 13 to 20 μs. While the restricted mobility index, introduced in Eq. (1), is able to capture the proportion of signal arising from the restricted mobility of solid, undissolved polymers in a sample, it is not possible to directly compare between samples with different polymer mass fraction, where there is a difference in the degree of dilution. Hence, when comparing solidity indices between formulations, over a range of dilutions, it is important to normalize the index, which we do so by dividing by the dilution factor originating from the addition of solvent protons. Where protonated solvents, such as water, are added, this dilution factor roughly corresponds to the concentration of the polymer (c_{poly}) in the sample, resulting in a normalized restricted mobility index, x_{norm}, based on polymer concentration (Eq. (2))

$$x_{norm} = \frac{x_u}{c_{poly}} \qquad \text{Eq. 2}$$

While, the correction in Eq. (2) is able to take into account the effect of added protons from a diluting solvent, it does not take into account the dependence of the NMR signal on the total number of protons, across all components in a sample, and not on the weight fraction of the polymer. This can be taken into account using the correction in Eq. (3), which determines a normalized restricted mobility index, x_p, based on the proportion of protons arising from the polymer.

$$x_p = \frac{x_u}{\frac{d_{p,poly} w_{poly}}{d_{p,poly} w_{poly} + d_{p,solv}\left(1 - w_{poly}\right)}} \qquad \text{Eq. 3}$$

where ($d_{p,poly}$) and ($d_{p,solv}$) are the "proton densities" of the polymer and solvent, respectively, which equate to number of protons per formula unit of each component, divided by each component's relative molecular weight, and the weight fraction of the polymer (w_{poly}) or solvent (1 – w_{poly}) in the sample. In samples with several liquid components, this equation can be generalized to give x_{p+}:

$$x_{p+} = \frac{d_{p,poly} w_{poly} + \sum d_{p,i} w_i}{d_{p,poly} w_{poly}} x_u \qquad \text{Eq. 4}$$

One last factor to include, when considering the polymer signal fraction, is the fact that some protons contained in a polymer might undergo fast exchange with the solvent phase and thus contribute to the solvent phase signal rather than to the polymer signal (or vice versa). In

this case, the correction needs to take this into account as well and we arrive at the following corrected equation for the proton-density corrected restricted mobility index (x_{pd}):

$$x_{pd} = \frac{d_{p,poly}w_{poly} + \sum d_{p,i}w_i}{d_{pne,poly}w_{poly}}x_u \quad \text{Eq. 5}$$

where $d_{pne,\ poly}$ is the density of non-exchanging protons in the polymer. The inclusion of $d_{p,i}$ and $d_{pne,\ poly}$ also supports the use of deuterated liquid phases, when comparing formulations which include, for example, D_2O, over a range of dilutions. While these deuterated phases are silent in the NMR signal decays, they need to be taken in account in terms of the exchangeable proton fractions and residual proton content when the different components are mixed together.

3. Results

A set of ^{1}H NMR SE-CPMG signal decay curves for a series of PVP samples can be found in Fig. 1. In the curves for samples with the highest PVP mass fractions ($\geq$0.767), an 'Abragam Oscillation' [22] can be seen, which is indicative of ordered or crystalline domains in a solid material [23], revealing the solid nature of PVP polymers in formulations with high mass fraction. For these samples, signal decays rapidly between 2 μs and 0.1 ms, which arises from protons in the polymer. There is significantly less decay between 0.1 and 1 ms, indicating the polymer is rigid, with restricted mobility for the protons within the polymer matrix. The remaining signal, arising from the solvent water protons, fully decays over a time scale of tens to hundreds of milliseconds. For PVP samples with mass fractions less than 0.603, there is negligible signal decay below 0.01 ms, indicating few or no solid-like protons remain. The signal decay over the timescale 0.02 – 1 ms are likely to arise from protons within a swollen polymer. As the mass fraction decreases, polymer solvation increases and hence there is an associated increase in the timescale over which the signal decays. Concurrently, the relaxation time of the water also increases significantly giving the lower relaxivity of the polymer.

In Fig. 2, ^{1}H NMR SE-CPMG signal decay curves are shown for a range of polyquat-37 samples, along with the 0.282 mass fraction sample of PVP, for comparison. It can be seen that for the neat polyquat-37 dispersion (0.50 mass fraction), the signal decays rapidly between 2 μs and 0.1 ms, with relatively no decay between 0.1 and 10 ms, before the signal fully decays with a significantly longer time constant. This initial, rapid decay is expected for dispersed solid (undissolved) polymers, which typically exhibit transverse relaxation times <20 μs [11], and is also observed in the aqueous PVP formulations with high polymer mass fraction ($\gtrsim$ 0.7). The slower decay arises from the continuous liquid phase, which exhibits an exponential decay with a time constant on the order of hundreds of ms. The 0.375 mass fraction polyquat sample, which is the next most concentrated polyquat sample, exhibits less signal decay below 20 μs, than neat polyquat, but shows a more continuous decay spanning 2 μs – 10 ms, which is indicative of strong plasticisation of the polymer [24,25]. For the remaining polyquat mixtures, with higher water content, their decay curves exhibit minimal decay below 0.1 ms, indicating the polymer is now mostly dissolved and hence demonstrating very little solid-like polymer. This is quite comparable to the 0.282 mass fraction PVP sample in which there is no undissolved polymer, where the corresponding SE-CPMG curves show no decay below 0.1 ms.

Multicomponent fitting was performed for each polyquat and selected PVP formulations. Plots showing these fits can be found in the supplementary information (Figs. S6 and S7), along with associated fitting parameters (Tables S1 and S2). From these fits, it can be seen that for a number of samples (0.50 and 0.375 polyquat-37 and 0.839, 0.767 and 0.676 PVP), a detectable proportion of undissolved polymer is observed, which exhibit a time constant $\leq$20 μs and can only be successfully fitted using a Gaussian function. A number of polyquat and PVP samples also show Gaussian components with longer time constants ($T_{2,gi} > 20$ μs), which are likely to arise from highly swollen polymers. All formulations require fitting with a range of exponential functions with time constants on the order of ms to s, which arise from more mobile dissolved polymers and water protons in the continuous phase.

In Fig. 3, we present the corrected restricted mobility indices (x_{pd}), determined using Eq. (5), for PVP formulations, along with the relaxation rate, $R_{2,water}$, for the water ($1/T_{2,water}$) divided by the polymer mass fraction. Both x_{pd} and $R_{2,water}$ increase with increasing polymer concentration. However, each plot exhibits transitions in behaviour, revealing three regimes for the state of dissolution of PVP, associated with dilute, semi-dilute and concentrated mixtures. In the more dilute PVP formulations (mass fractions $\lesssim$ 0.4), the polymer is fully dissolved. Water molecules interacting with the polymer will have a higher relaxation rate compared to bulk water. These water molecules will be in

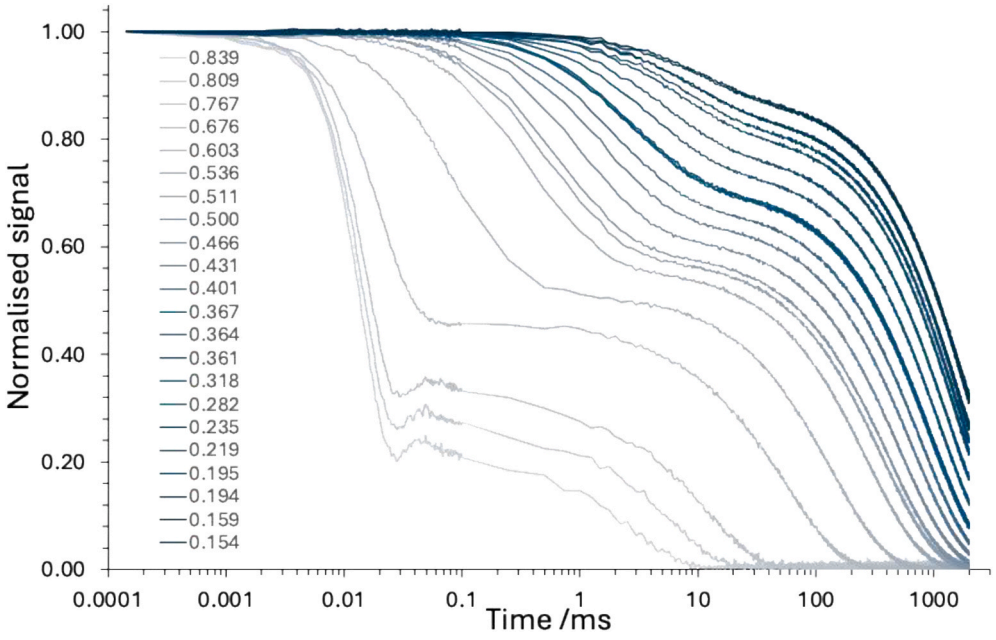

Fig. 1. ^{1}H SE-CPMG NMR data, recorded at 30 °C, for a range of PVP:water mixtures, over polymer mass fractions of 0.154 – 0.839.

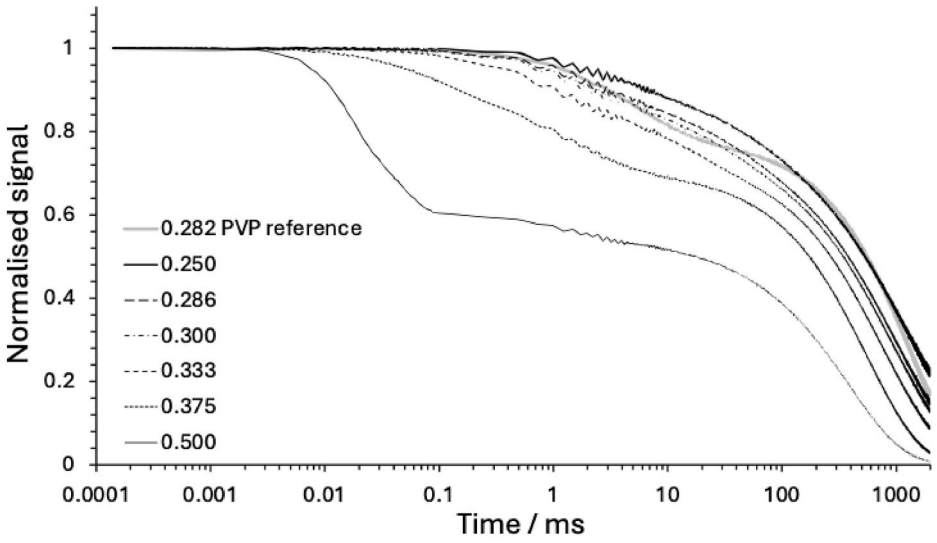

Fig. 2. ^{1}H SE-CPMG NMR data, recorded at 30 °C, for a range of polyquaternium-37 mixtures, with polymer mass fractions in the range of 0.25 – 0.50, and a PVP reference solution with a mass fraction of 0.282.

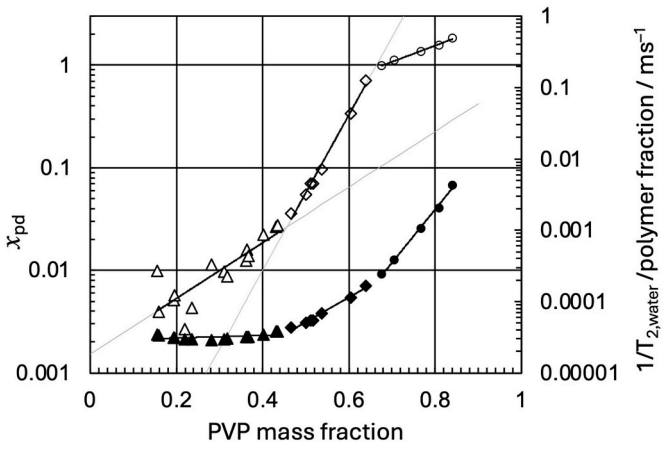

Fig. 3. Plot of the proton-density corrected restricted mobility index, x_{pd}, (open symbols) and the relaxation rate of water ($1/T_{2,water}$) divided by the polymer fraction (closed symbols) as a function of PVP mass fraction, determined using the SE-CPMG decay curves for the PVP:water mixtures in Fig. 1.

fast exchange with bulk water, resulting in a single relaxation rate. In this dilute regime, the relaxation rate for water ($R_{2,water}$) is expected to scale linearly with the polymer fraction (w_{poly}) [26]. Hence, the ratio between the $R_{2,water}$ and w_{poly} is expected to be constant [26–28], which is what is observed for the samples plotted as triangles. As the polymer mass fraction increases, the solution becomes semi-dilute and the slope of the relaxation rate of water increases more steeply with mass fraction. This is because the hydrated polymer chains come into direct contact with each other and there is a subsequent reduction in their mobility, as well as the mobility of interacting water molecules. This increasing relaxation rate is observed in Fig. 3 for the PVP solutions plotted as diamonds. Lastly, in the concentrated regime, there are a greater number of contacts between polymer chains and hence fewer water molecules are able to associate with individual chains, reducing the mobility of polymers further, and subsequently the rate of increase in relaxation rate for the associated water molecules. Hence, there is a further transition in the rate at which the relaxivity changes with polymer fraction, which is observed for the aqueous PVP formulations with high polymer mass fraction, plotted as circles (at mass fractions $\gtrsim 0.7$). What is observed in the relaxation rate of water, is mirrored in the plot of the corrected restricted mobility index. In the dilute polymer formulations, where the polymer is fully dissolved and has greatest mobility, x_{pd} is expected to be low, which is what is observed for the samples plotted as triangles. As the polymer increases into the semi-dilute regime, plotted as diamonds (for mass fractions $\lesssim 0.4$), an increase in the slope of x_{pd} vs w_{poly} is observed, associated with the reduced mobility of protons. The restricted mobility index at which the transition occurs, which marks the point at which the polymer chains are no longer fully solvated, is $x_{pd} = 0.026$ (where the trendlines for dilute and semi-dilute regimes intersect). The transition to the concentrated regime is observed at a mass fraction of 0.676, at a restricted mobility index around 1. At this mass fraction, and above, it is expected from x_{pd} that solid (undissolved) polymer components are present. This observation is matched in the multicomponent fits for these samples (Fig. S8 and Table S2, in the Supplementary Information), which show that these same formulations also exhibit signal decays with a time constant $\leq$20 μs, which is expected for materials comprising solid/undissolved components.

In Fig. 4, we present the corrected restricted mobility indices, from Eq. (5), for different dilutions of a neat polyquaternium-37 dispersion with water, at different temperatures. The corrected restricted mobility index at the point where PVP polymers are no longer fully solvated at 30 °C (determined from the plot in Fig. 3), is shown as the dashed grey line in the plot. The corrected restricted mobility indices (x_{pd}) and associated fitting parameters for these formulations, at 30 °C and 50 °C, are presented in Tables S3 and S4 in the Supplementary Information. While restricted mobility indices for the neat polyquat-37 formulation (at a polyquat mass fraction of 0.5) exhibit almost no temperature dependence, the corrected restricted mobility indices of diluted samples show a reduction in the value of the index with decreasing polymer content and increasing temperature. This plot is able to demonstrate that at 30 °C, there is a comparable degree of restricted mobility in the 0.3 mass fraction polyquat sample, as there is at the restricted mobility index where PVP polymers are no longer fully solvated (where $x_{pd} = 0.026$, corresponding to a PVP mass fraction of 0.46). Moreover, for the polyquat sample with a mass fraction of 0.333, the temperature at which the restricted mobility index matches that of the PVP reference is 40 °C (Table S4). This can be seen more easily in the inset plot, which plots the corrected restricted mobility indices logarithmically.

To demonstrate the general applicability of this approach, we monitored the solubilisation of cellulose using the restricted mobility index. In Fig. 5, signal decay curves are shown, using a treatment strategy based on NaOH and low temperatures [29]. Solutions of 8% cellulose in 8% NaOH dissolved in D_2O processed over a variable

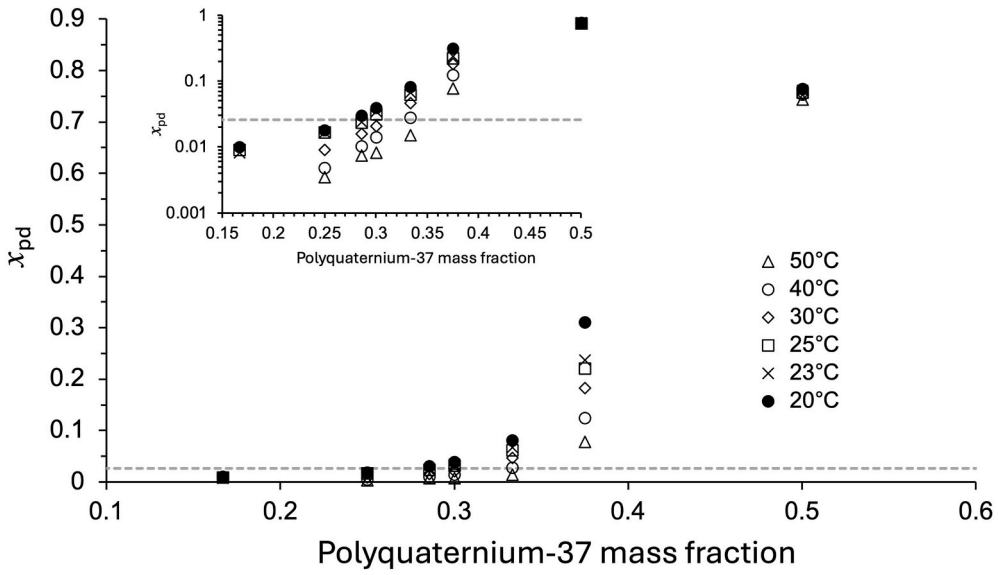

Fig. 4. Corrected restricted mobility index (x_{pd}) calculated from SE-CPMG decay curves for polyquaternium-37 dispersion diluted with different amounts of water and measured at different temperatures. The PVP sample was measured at 30 °C. The inset plot shows the corrected restricted mobility indices on a logarithmic scale for polyquaternium-37 samples for mass fractions between 0.15 and 0.4. The dashed line indicates the corrected restricted mobility index at 0.026, determined from the PVP samples (Fig. 3) as the value at which the polymer is no longer fully solvated.

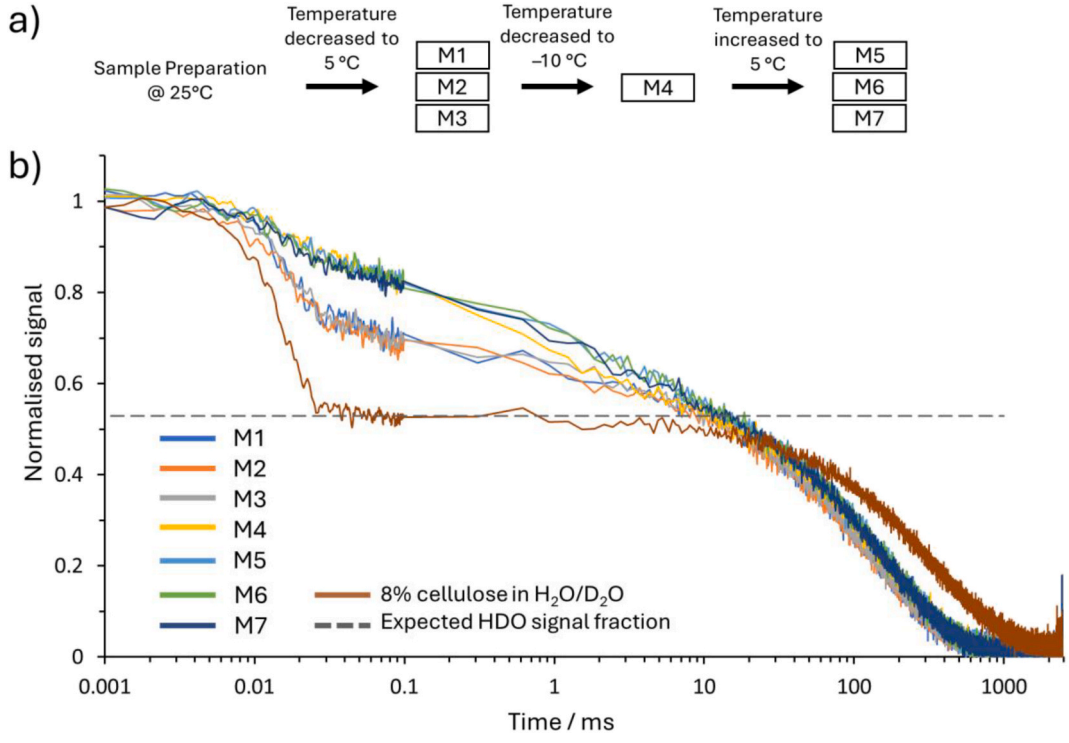

Fig. 5. a) A schematic diagram showing the temperature and relaxation curve measurement scheme for experiments samples of 8% cellulose (MCC) in 8% NaOH in D_2O sample. Each measurement (M1 – M7) took 10 min to acquire, with measurements (M1-3 and M5-7) at both 5 °C stages acquired 20 min apart. b) Signal decay curves collected at the temperature and order indicated in part (a) for 8% cellulose in 8% NaOH in D_2O sample at 5 °C before and after −10 °C treatment and 8% cellulose in 8% H_2O in D_2O.

temperature scheme, which is represented graphically in Fig. 5a. The first three measurements (M1-3) were collected at a temperature of 5 °C, before the temperature was decreased to −10 °C and a single measurement (M4) was collected, followed by a temperature increase back to 5 °C before the final three measurements (M5-7) were collected. The measurements (M1-M7) were performed on the same sample. A reference sample is included, comprising the same cellulose powder in a mixture of 1.8% H_2O with 98.2% D_2O (corresponding to the proton content in 8% NaOH). The corresponding restricted mobility indices for these signal decays, were calculated using Eq. (5) and are presented in Fig. 6.

Lastly, to test whether dilution with D_2O, rather than H_2O, significantly affects the relaxation behaviour of the polymeric components, and hence the restricted mobility index, particularly where there are a

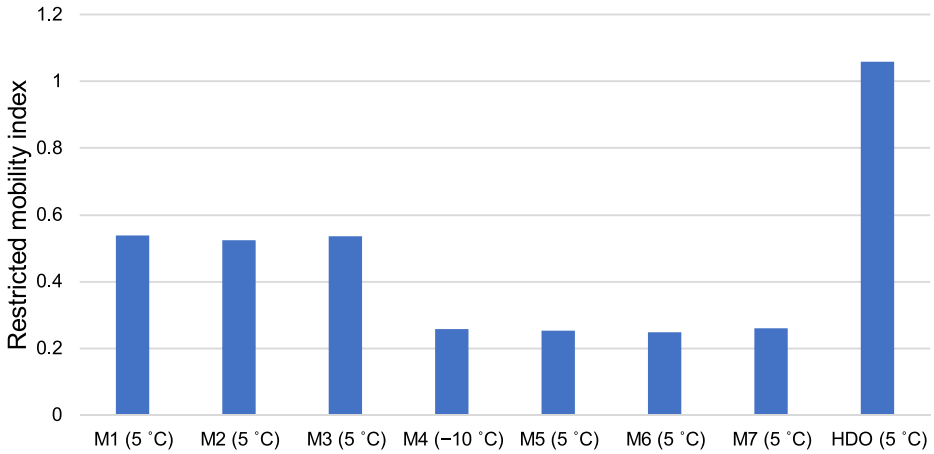

Fig. 6. Restricted mobility indices for 8% cellulose (MCC) in 8% NaOH in D_2O collected, for the relaxation curves presented in Fig. 5(b), in the order, and at the temperature, indicated in the measurement scheme shown in Fig. 5(a).

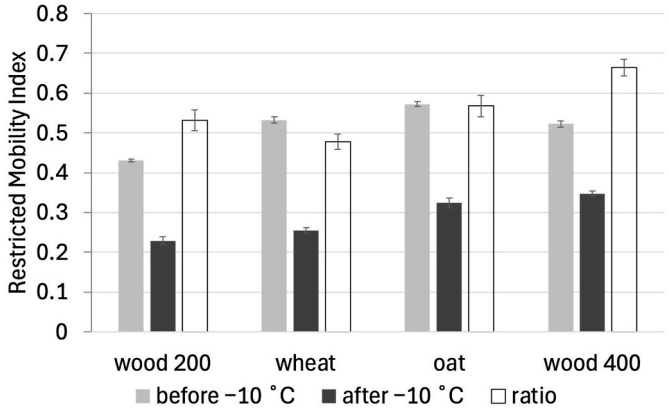

Fig. 7. restricted mobility index before and after −10 °C treatment and ratio of the index after and before for cellulose from a range of different sources.

significant number of exchangeable protons, the relaxation curves for two samples of cellulose were collected. One diluted with H_2O, the other with D_2O. These two plots are presented as raw signal decays (Fig. S10) and normalized signal decays (Fig. 8), where the ^1H signal from solvent has been subtracted. These two samples are expected to contain a high degree of solid-like polymer, with a correspondingly high amount of signal decay <20 μs. These plots show this behaviour, as well as nearly identical polymer signals for both samples, regardless whether the dilution was with D_2O or H_2O, leading to comparable restricted mobility indices for each sample.

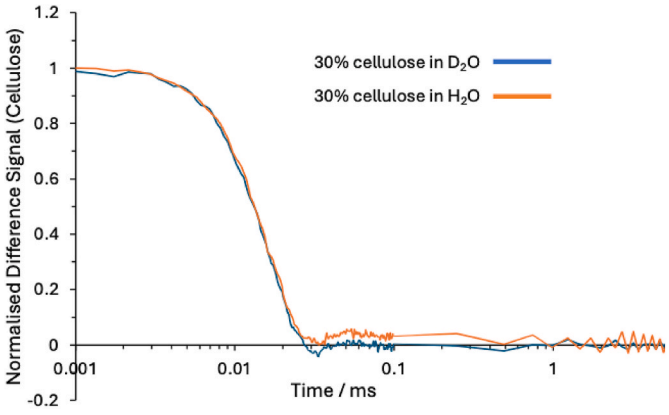

Fig. 8. The normalized difference signal for solutions of 30% cellulose (MCC) in H_2O and D_2O.

4. Discussion

Multicomponent fitting of the relaxation time decays for the synthetic polymers PVP and polyquaternium-37 (Figs. S6 and S7; Tables S1 and S2), revealed multiple time constants, with values on the order of 20 μs, or less, for immobile (undissolved) polymeric components, >0.02 μs for more mobile swollen polymer components and >100 ms for the solvent (Tables S1 and S2). While a minimum number of components were employed (which achieved an R^2 value of ≥0.995) in each multicomponent fitting, all samples required a minimum of two components, with many of them requiring four or more, as well as a combination of Gaussian and exponential functions. These multicomponent fits were able to detect changes in the degree of restricted mobility species and assess the relative contributions from immobile dispersed solids and more mobile components. It was found that where formulations exhibited a discernible signal decay (≥1%) below 0.1 ms, a combination of both Gaussian and exponential functions were required to fit the data. In formulations where there was no discernible decay below 0.1 ms, only exponential functions were required to fit the data. While these multicomponent fits were able to successfully fit each of the decay curves, they highlight the challenges of using multicomponent fitting to characterize complex formulations. In particular, such fitting is highly subjective to the number and nature of the functions used and their starting values and fits with several time constants are unlikely to be unique solutions. Hence, there is a high-level of subjectivity in these fitting parameters. In addition to the sensitivity and subjectivity of multicomponent fitting, as is also often observed using inverse Laplace transforms, these methods do not return a single characterising parametric quantity, are time intensive and require a level of operator input, making it hard to automate or translate this type of analysis. Hence, in order to assess the degree of undissolved polymer, or otherwise immobile polymeric components, within a formulation, a more robust characterization tool is required, which is easy to implement and less subjective. To this end, the restricted mobility index was developed which quantifies the degree of solid/undissolved, immobile polymer components within a formulation. Using the restricted mobility index, we present a model-free approach for quantifying the level of undissolved (solid) polymer components within a formulation, for the first time, and demonstrate this is affected by the nature of the polymer, its level of dilution and its temperature. While the observed behaviour of polymers within these formulations is not unexpected, we have been able to, for the first time, provide a simple and robust method by which the level of solid content can be quantified and make it possible to

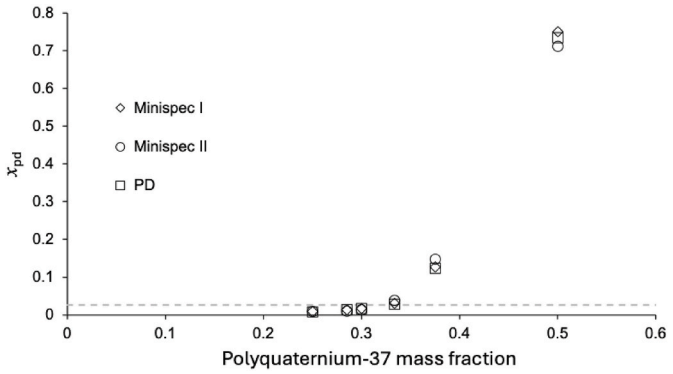

Fig. 9. Corrected restricted mobility indices calculated from SE-CPMG decay curves for polyquaternium-37 mixtures measured at 40 °C on three different instruments, two Bruker minispec mq20 spectrometers and a Pure Devices magspec NMR-SCA. The dashed line indicates the corrected restricted mobility index at 0.026, determined from the PVP samples (Fig. 3) as the value at which the polymer is no longer fully solvated.

objectively compare this level between different formulations.

In the case of PVP, we are able to reveal dilute, semi-dilute and concentrated regimes for the formulations studied and identify the mass fractions at which transitions between these regimes occur. For the polyquat-37 formulations, it is possible to detect a transition from partly undissolved to fully-dissolved polymer at a mass fraction $\leq$0.333, at a temperature of 50 °C. While at 25 °C, this transition occurs at mass fractions below 0.25. This transition in polymer character is not obvious from the macroscopic physical appearance of these samples (see Fig. S1 in the supplementary information), which are all, with the exception of the 0.375 mass fraction sample, strongly turbid to opaque. Not only is the appearance of these samples unable to provide a measure of the physical state of components within the sample, their turbidity also makes analysis of these sample challenging using optical analytical methods. Furthermore, macroscopic flow behaviour has also been found to not directly correlate with the change physical state of components, as measured by the restricted mobility index. The flowability for each of the polyquat samples was tested by placing each sample tube on its side and can be observed from the degree to which each formulation is able to spread through each tube, as shown in the photo in Fig. S1. In these flowability tests, the neat sample and 0.375 mass fraction sample exhibit a small level of deformation, the samples at mass fractions of 0.333 and 0.3 demonstrate they are highly flowable. Only the samples at mass fractions of 0.286 and 0.25 exhibit negligible flowability. These flowability results demonstrate there is no link between the level of solid-like components within a formulation and its macroscopic flow behaviour. This observation may not be surprising, as NMR relaxation is mainly dependent on effects happening at a molecular distance and the flow behaviour is strongly dependent on effects happening over a micrometre length scale, and longer. However, it is another example of the difficulty of finding a simple test to determine the physical state of components within a formulation.

To demonstrate the general applicability of our approach, we extended the application of the method to characterize another polymeric material. Cellulose was selected because it is harder to fully dissolve, making these natural polymeric solutions more challenging to characterize. Formulations comprising these types of polymers are further complicated by the contribution of a higher proportion of exchangeable protons and unknown or uncontrolled levels of water content. Cellulose formulations can be further complicated by the presence of additives, such as NaOH, which is often used to modify polymer formulations and is known to change the dissolution state of cellulose, especially at low temperatures [29]. In the relaxation curves (Fig. 5) of cellulose we are able to reveal the effects of the Sobue treatment of cellulose on a cellulose solution, compared to that of a reference sample of 8% cellulose in H_2O/D_2O. The sample containing NaOH (curves M1-3) shows less signal decay <100 μs than the reference cellulose, indicating greater swelling of the cellulose. Moreover, following an increase in temperature from −10 °C to 5 °C (curves M5-7), the cellulose has macroscopically changed, from a swollen polymeric material to a viscous solution. What the restricted mobility indices in Fig. 6 are able to reveal is that cellulose becomes more mobile on the addition of NaOH and more mobile still following a decrease in temperature, compared to only diluting with HDO. These data show that by lowering the temperature, the hydrophobic interactions are weakened and cellulose becomes more fully dissolved and hence more mobile, which remains the case even after increasing the temperature again. Following the addition of NaOH and this temperature scheme, the cellulose sample becomes, more or less, a homogeneous, transparent viscous solution. The restricted mobility index is able to act as an indicator of the effect of the drop in temperature step, to −10 °C , for how well different cellulose grades respond to the Sobue mobilization effect [29,30], as well as a means of validating the effect of different additives on this mobilization. In Fig. 6, a comparison of four different cellulose sources and processing, which have been subjected to the same protocol, is presented. The ratio presented in Fig. 7, between the indices before and after the low-temperature treatment, provides a means by which to assess the effectiveness of this low-temperature treatment on the degree of dissolution of different cellulose grades or preparations with different additives.

Finally, the robustness of this approach and broad-applicability of these measurements are demonstrated in the comparison of restricted mobility indices determined using different instruments, across multiple labs. In Fig. 9, the restricted mobility indices for polyquat-37 sample mixtures are shown, measured across three different instruments in different locations. The plot shows excellent agreement for the indices at each polyquat-37 dilution, demonstrating the reproducibility of the measurement on different devices and the robust nature of the methodology.

5. Conclusions

Using the restricted mobility index, we have been able to quantify, for the first time, the degree of undissolved (solid), or partially dissolved, polymer content within a complex polymeric formulation and have been able to compare these levels between different formulations, over a range of different temperatures. In this paper, we have applied the method to study polymer formulations. However, this approach can also be employed to monitor polymer degradation, the assessment of the loss of solid plastics in biodegradation and polymer recycling strategies. The method is rapid and easy to implement and does not suffer from the same level of subjectivity or sensitivity as traditional methods for probing the behaviour of multicomponent mixtures, such as multicomponent fitting or inverse Laplace transforms. Furthermore, what the restricted mobility index offers is a simple and easy to implement approach, which is universal and easily transferable and automatable. As a result, this index is capable of the rapid assessment of the solution state of polymers in disperse systems, paving the way for the regulatory assessment of polymer-containing products, the assessment of formulation stability and the determination of the degree of dissolution, or even melting, of polymers across a range of technical processes.

Funding sources

The authors thank BASF SE, Germany for financial support.

CRediT authorship contribution statement

Joseph U. Okeke: Formal analysis, Investigation, Methodology, Visualization, Writing – original draft. **Festus Slade:** Investigation, Methodology, Writing – review & editing. **Dietmar Obst:**

Conceptualization, Resources, Supervision. **Diana Bernin:** Investigation, Writing – review & editing. **Nikolaus Nestle:** Conceptualization, Formal analysis, Investigation, Methodology, Resources, Supervision, Writing – original draft. **Melanie M. Britton:** Investigation, Methodology, Supervision, Writing – original draft.

Declaration of competing interest

The authors declare the following financial interests/personal relationships which may be considered as potential competing interests: Melanie Britton reports financial support and equipment, drugs, or supplies were provided by BASF SE. Joseph Okeke reports financial support was provided by BASF SE. Festus Slade reports financial support was provided by BASF SE. If there are other authors, they declare that they have no known competing financial interests or personal relationships that could have appeared to influence the work reported in this paper.

Appendix A. Supplementary data

Supplementary data to this article can be found online at https://doi.org/10.1016/j.jciso.2026.100185.

Data availability

The data generated in this study are available at https://doi.org/10.25500/edata.bham.00001505.

References

[1] G. Satchanska, S. Davidova, P.D. Petrov, Natural and synthetic polymers for biomedical and environmental applications, Polymers 16 (2024) 1159, https://doi.org/10.3390/polym16081159.

[2] A.C.Q. Silva, A.J.D. Silvestre, C. Vilela, C.S.R. Freire, Natural polymers-based materials: a contribution to a greener future, Molecules 27 (2021) 94, https://doi.org/10.3390/molecules27010094.

[3] A. Rohani Shirvan, A. Nouri, A. Sutti, A perspective on the wet spinning process and its advancements in biomedical sciences, Eur. Polym. J. 181 (2022) 111681, https://doi.org/10.1016/j.eurpolymj.2022.111681.

[4] ASTM D4359-90, Standard test method for determining whether a material is a liquid or a solid. https://doi.org/10.1520/D4359-90R24, 2024.

[5] OECD, Test No. 120: solution/extraction behaviour of polymers in water. OECD Guidelines for the Testing of Chemicals, Section 1, OECD Publishing, Paris, 2000, https://doi.org/10.1787/9789264069886-en.

[6] J. Gummel, Y. Roiter, V. Agostiniano, K. Goodall, E. Fratini, Defining the conformation of water-soluble Poly(vinyl alcohol) in solution: a SAXS, DLS, and AFM Study, ACS Omega 10 (2025) 18840–18847, https://doi.org/10.1021/acsomega.5c00692.

[7] M.F. Cobo, E.J. Deublein, A. Haber, R. Kwamen, M. Nimbalkar, F. Decker, TD-NMR in quality control: standard applications, in: G.A. Webb (Ed.), Modern Magnetic Resonance, Springer International Publishing, Cham, 2018, pp. 1819–1836.

[8] D. Besghini, M. Mauri, R. Simonutti, Time domain NMR in polymer science: from the laboratory to the industry, Appl. Sci. 9 (2019) 1801, https://doi.org/10.3390/app9091801.

[9] B. Ozel, M.H. Oztop, A quick look to the use of time domain nuclear magnetic resonance relaxometry and magnetic resonance imaging for food quality applications, Curr. Opin. Food Sci. 41 (2021) 122–129, https://doi.org/10.1016/j.cofs.2021.03.012.

[10] F. Dalitz, M. Cudaj, M. Maiwald, G. Guthausen, Process and reaction monitoring by low-field NMR spectroscopy, Prog. Nucl. Magn. Reson. Spectrosc. 60 (2012) 52–70, https://doi.org/10.1016/j.pnmrs.2011.11.003.

[11] A. Maus, C. Hertlein, K. Saalwächter, A robust proton NMR method to investigate hard/soft ratios, crystallinity, and component mobility in polymers, Macromol. Chem. Phys. 207 (2006) 1150–1158, https://doi.org/10.1002/macp.200600169.

[12] S.S. Uguz, B. Ozel, L. Grunin, E.B. Ozvural, M.H. Oztop, Non-Conventional Time Domain (TD)-NMR approaches for food quality: case of gelatin-based candies as a model food, Molecules 27 (2022), https://doi.org/10.3390/molecules27196745.

[13] L. Grunin, M.H. Oztop, S. Guner, S.F. Baltaci, Exploring the crystallinity of different powder sugars through solid echo and magic sandwich echo sequences, Magn. Reson. Chem. 57 (2019) 607–615, https://doi.org/10.1002/mrc.4866.

[14] O. Tas, U. Ertugrul, L. Grunin, M.H. Oztop, Investigation of the hydration behavior of different sugars by time Domain-NMR, Foods 11 (2022), https://doi.org/10.3390/foods11081148.

[15] R. Lamanna, On the inversion of multicomponent NMR relaxation and diffusion decays in heterogeneous systems, Concepts Magn. Reson. A 26a (2005) 78–90, https://doi.org/10.1002/cmr.a.20036.

[16] K.P. Whittall, A.L. Mackay, Quantitative interpretation of nmr relaxation data, J. Magn. Reson. 84 (1989) 134–152, https://doi.org/10.1016/0022-2364(89)90011-5.

[17] R.L. Parker, Y.Q. Song, Assigning uncertainties in the inversion of NMR relaxation data, J. Magn. Reson. 174 (2005) 314–324, https://doi.org/10.1016/j.jmr.2005.03.002.

[18] J. Wojtasz, J. Bengtsson, H. Ulmefors, D. Bernin, Å. Östlund, S. Yu, In-situ X-ray analysis of cold alkali dissolution of cellulose pulps of various origin, Cellulose 32 (2024) 115–131, https://doi.org/10.1007/s10570-024-06235-7.

[19] N. Nestle, K. Haberle, Non-invasive analysis of swelling in polymer dispersions by means of time-domain(TD)-NMR, Anal. Chim. Acta 654 (2009) 35–39, https://doi.org/10.1016/j.aca.2009.05.001.

[20] MATLAB Version: 24.1.0.2568132 (R2024A) Update 1, The MathWorks Inc., 2024.

[21] B. Blümich, J. Perlo, F. Casanova, Mobile single-sided NMR, Prog. Nucl. Magn. Reson. Spectrosc. 52 (2008) 197–269, https://doi.org/10.1016/j.pnmrs.2007.10.002.

[22] A. Abragam, The Principles of Nuclear Magnetism, Clarendon Press, Oxford, 1961.

[23] V. Räntzsch, M. Haas, M.B. Özen, K.-F. Ratzsch, K. Riazi, S. Kauffmann-Weiss, J. K. Palacios, A.J. Müller, I. Vittorias, G. Gisela, M. Wilhelm, Polymer crystallinity and crystallization kinetics via benchtop 1H NMR relaxometry: revisited method, data analysis, and experiments on common polymers, Polymer 145 (2018) 162–173, https://doi.org/10.1016/j.polymer.2018.04.066.

[24] R.R. Bavin, D.I. Fursov, S.G. Vasil'ev, V.P. Tarasov, V.A. Zabrodin, V.I. Volkov, Features of rubber swelling in transformer oil, according to NMR data, Russ. J. Phys. Chem. A 90 (2016) 1650–1655, https://doi.org/10.1134/s0036024416080033.

[25] H. Hatakeyama, T. Hatakeyama, Interaction between water and hydrophilic polymers, Thermochim. Acta 308 (1998) 3–22, https://doi.org/10.1016/s0040-6031(97)00325-0.

[26] M.Z. Jora, M.V.C. Cardoso, E. Sabadini, Dynamical aspects of water-poly(ethylene glycol) solutions studied by 1H NMR, J. Mol. Liq. 222 (2016) 94–100, https://doi.org/10.1016/j.molliq.2016.06.101.

[27] N. Nestle, F. Quero, Z. Xu, M. Bencsik, Unusual increase of apparent transverse relaxation times in NMR profiling of a drying polymer solution, Appl. Magn. Reson. 45 (2014) 1311–1317, https://doi.org/10.1007/s00723-014-0600-0.

[28] E. Sabadini, F.D. Egídio, F.Y. Fujiwara, T. Cosgrove, Use of water spin-spin relaxation rate to probe the solvation of cyclodextrins in aqueous solutions, J. Phys. Chem. B 112 (2008) 3328–3332, https://doi.org/10.1021/jp710013h.

[29] H. Sobue, H. Kiessig, K. Hess, Das System Cellulose–Natriumhydroxyd–Wasser in Abhängigkeit von der Temperatur, Z. Phys. Chem. 43B (1939) 309–328, https://doi.org/10.1515/zpch-1939-4324.

[30] M. Gunnarsson, M. Hasani, D. Bernin, The potential of magnetisation transfer NMR to monitor the dissolution process of cellulose in cold alkali, Cellulose 26 (2019) 9403–9412, https://doi.org/10.1007/s10570-019-02728-y.